I&EC research
Industrial & Engineering Chemistry Research

Article

Cite This: Ind. Eng. Chem. Res. XXXX, XXX, XXX−XXX

pubs.acs.org/IECR

Monitoring the Enzymatic Oxidation of Xenobiotics by Hydrogen Peroxide through Oxidation−Reduction Potential Measurements

D. A. Morales Urrea,[†] P. M. Haure,[†,‡] and E. M. Contreras*[,†]

[†]Instituto de Investigaciones en Ciencia y Tecnología de Materiales (INTEMA), CCT - Mar del Plata CONICET, Av Juan B. Justo 4302, 7600 Mar del Plata, Argentina

[‡]Departamento de Ingeniería Química, Facultad de Ingeniería, Universidad Nacional de Mar del Plata (UNMdP). Av Juan B. Justo 4302, 7600 Mar del Plata, Argentina

Supporting Information

ABSTRACT: In this work, three xenobiotics (orange II, phenol, and bisphenol A) were oxidized by hydrogen peroxide in the presence of a horseradish peroxidase (HRP) using a fed-batch system. During the experiments, the oxidation−reduction potential (ORP) of the reaction mixture was measured continuously. Results demonstrate that ORP values only increased when both substrates of the enzyme (hydrogen peroxide and the target compound) were present in the reaction mixture. For all of the tested pollutants, the continuous addition of hydrogen peroxide caused an increase in ORP values. When the reducing substrate was depleted, the addition of an excess of hydrogen peroxide caused a decrease of ORP values. The time at which ORP reached a maximum represented the end of the oxidation process. This maximum could be easily detected by means of the derivative of ORP as a function of time. To extend the application of the developed technique, the enzymatic oxidation of a binary mixture of BPA and OII was also followed using ORP measurements. Results were similar to those observed with only one reducing substrate. This work demonstrates that ORP measurements can be useful to maximize hydrogen peroxide efficiency through the controlled addition of the oxidant during the oxidation of OII, phenol, and BPA catalyzed by HRP. This approach allows a minimization of time and process costs since the reaction end-point can be easily detected on a real-time basis.

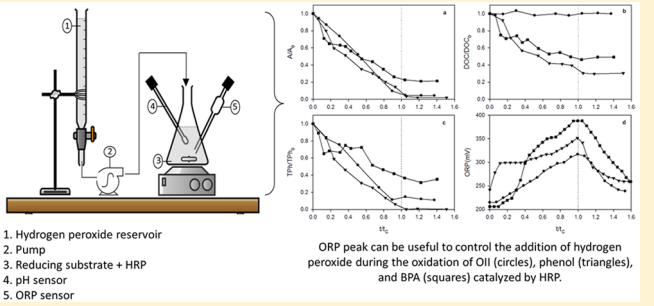

1. INTRODUCTION

Biochemically assisted degradation processes are based on the metabolic potential of microorganisms or their enzymes to degrade a wide variety of compounds.[1] The major drawback of using microorganisms is the fact that the removal process may take longer due to acclimation issues and is less predictable in comparison with physicochemical methods. However, the use of enzymes instead of microorganisms is a simple way to obtain high removal rates of a specific compound under predictable conditions.[2] Additionally, enzymatic degradation is preferred in cases where the target compound inhibits the microbial growth. For this reason, the enzymatic removal of organic compounds could be an eco-friendly cost-competitive alternative compared to physicochemical or microbiological methods.[1,3,4] In particular, the use of peroxidases (e.g., soybean peroxidase, manganese peroxidase, lignin peroxidase, and horseradish peroxidase) or their biomimetic systems (e.g., hematin) has been tested to oxidize several xenobiotic compounds.[2,5−8]

One of the main costs associated with the removal of xenobiotics using peroxidases is related to the use of hydrogen peroxide as the oxidant. Many mathematical models regarding the effect of the initial concentration of hydrogen peroxide, target substrates, and pH on the activity of peroxidases can be been found in the literature. Among those models, the Dunford mechanism is the most referenced.[2,9,10] According to this mechanism, 2 mol of the reducing compound (S) can be oxidized per mole of hydrogen peroxide consumed. However, this value is difficult to achieve because peroxidases in the presence of a reducing substrate also catalyze the decomposition of hydrogen peroxide to oxygen and water.[7,11,12] Moreover, in a recent work, Morales Urrea et al.[13] demonstrate that the decomposition of hydrogen peroxide catalyzed by a horseradish peroxidase increases with the initial hydrogen peroxide concentration.

A simple way to maximize hydrogen peroxide efficiencies in terms of moles of the reducing compound oxidized per mole of hydrogen peroxide consumed is the dropwise addition of the oxidant, such as in fed-batch reactors. The optimal operation of a fed-batch requires a careful tuning of concentrations and flow rates. For a given reducing substrate (S) concentration, high enzyme concentrations and low P input rates should favor low hydrogen peroxide concentrations. This approach will reduce

Received: September 20, 2018
Revised: November 7, 2018
Accepted: November 12, 2018
Published: November 12, 2018

DOI: 10.1021/acs.iecr.8b04616
Ind. Eng. Chem. Res. XXXX, XXX, XXX−XXX

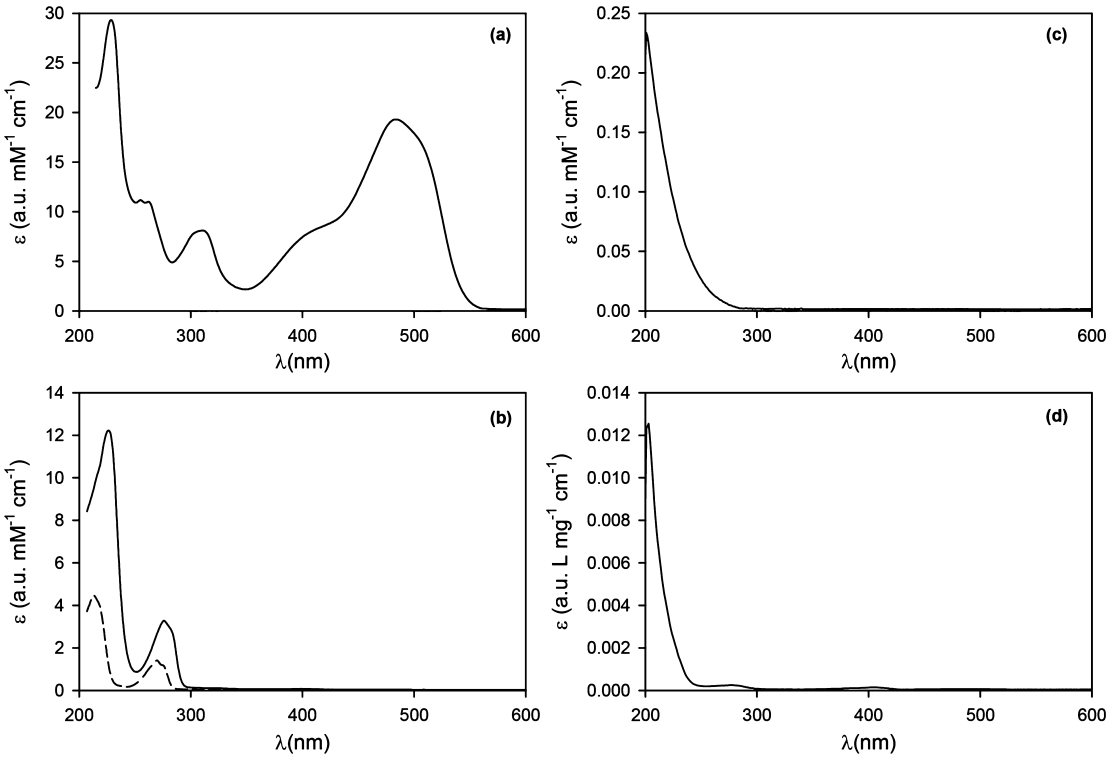

Figure 1. Molar attenuation coefficient (ε) at pH 8 in phosphate buffer (100 mM) as a function of wavelength (λ) corresponding to (a) Orange II, (b) BPA (continuous line) and phenol (dashed line), (c) hydrogen peroxide, and (d) HRP.

the parasitic decomposition of hydrogen peroxide, enhancing the consumption efficiency in terms of moles of substrate oxidized per mol of hydrogen peroxide consumed (Y_S). Therefore, a key point to avoid the addition of an excess of hydrogen peroxide is to detect the depletion of the reducing substrate. If target compounds are depleted then the addition of hydrogen peroxide is useless, increasing the spend of oxidant, operation time, and the overall cost of the process.

Several authors propose the use of oxidation−reduction potential (ORP) measurements to monitor the oxidation of several xenobiotics using advanced oxidation processes.[14−16] Although ORP measurements were recently used to monitor several biological wastewater treatment processes,[17−21] to our knowledge, the use of ORP to monitor an enzymatic system to remove xenobiotics has not been proposed in the literature. For this reason, in this contribution a method to of the HRP mediated oxidation of three model pollutants (orange II, phenol, and bisphenol A) with fed-batch addition of hydrogen peroxide based on ORP measurements was developed.

2. MATERIALS AND METHODS

2.1. Chemicals and Reagents. Azo dye Orange II (OII) sodium salt (CAS no. 633-96-5), phenol (CAS no. 108-95-2), BPA (CAS no. 80-05-7), and horseradish peroxidase (HRP) Type I (CAS no. 9003-99-0) were obtained from Sigma-Aldrich. The enzyme was supplied as a lyophilized powder, and it was used without further purification. According to the manufacturer, the specific activity was 146 units/mg of the solid powder (one unit corresponds to the amount of enzyme that forms 1 mg of purpurogallin from pyrogallol in 20 s at pH 6 and 20 °C). All other salts used in this work were reagent grade from Anedra (San Fernando, Argentina).

2.2. Experimental Setup and Methods. Oxidation assays were performed in 250 mL beakers at room temperature (20 ± 2 °C). Appropriate amounts of HRP and the tested compounds (OII, phenol, BPA) were diluted in a phosphate buffer (100 mM) at the tested pH. Hydrogen peroxide stock solutions were prepared using the same phosphate buffer. For the fed-batch operation, a peristaltic pump (Apema model PC25-1-M6-S) was used to fed dropwise hydrogen peroxide stock solutions of appropriate concentrations (P_{in}) with different flow rates. Tested HRP concentrations ranged from 20 to 30 mg/L. ORP and pH were continuously measured using polymer body probes (Broadley-James Corp., USA). An 8-bit A/D converter (Biloba Ingenieria, model BLB 2.0) was used to obtain the output signal (4−20 mA) from both monitors. The A/D converter module was connected to a personal computer via a RS232 protocol. At appropriate intervals, samples were withdrawn from the reactor. These samples were immediately centrifuged for 5 min at 13000 rpm (Eppendorf 5415C), and the supernatant was filtered through 0.45 mm cellulosic membranes (Osmonics, Inc.). Then appropriate dilutions of the filtrates were performed using the above-mentioned phosphate buffer (100 mM), and UV/vis spectra were recorded using a spectrophotometer Shimadzu UV-1800. Dissolved organic carbon (TOC) of these dilutions was also measured in a Shimadzu TOC-VCPN analyzer. When phenol or BPA was tested, the total phenol concentration (TPh) was measured using the 4-aminoantipyrine (4-AAP) method.[22] In this method, 4-AAP (20.8 mM of 4-AAP in 0.25 M $NaHCO_3$) and ferricyanide (83.4 mM of $K_3Fe(CN)_6$ in 0.25 M $NaHCO_3$) are color-generating substrates when combined with phenolic compounds. These colored complexes were measured at 510 nm. Calibration curves were performed periodically using phenol or BPA as the reference compounds.

DOI: 10.1021/acs.iecr.8b04616
Ind. Eng. Chem. Res. XXXX, XXX, XXX−XXX

3. RESULTS AND DISCUSSION

3.1. UV/vis Spectra of the Tested Compounds. Figure 1 shows the molar attenuation coefficient (ε) at pH 8 corresponding to OII (Figure 1a), BPA and phenol (Figure 1b), hydrogen peroxide (Figure 1c), and the HRP employed in the present work (Figure 1d). With regard to the tested dye, according to several authors,[23,24] the absorption bands at 485 and 430 nm correspond to the OII hydrazone and azo tautomeric forms, respectively. The other two bands at 230 and 310 nm are related to the benzene and naphthalene rings of OII. In addition, BPA and phenol had similar spectra, presenting two absorption bands at around 275 and 215 nm. Considering the highest initial peroxide (0.21 mM) and enzyme (30 mg/L) concentrations tested in the present work, and according to the molar attenuation coefficients depicted in Figure 1, for wavelengths higher than 240 nm absorbances corresponding to hydrogen peroxide and HRP were less than 0.01. Because these absorbances were negligible in comparison with those corresponding to OII, BPA, or phenol (Figure S1), absorbance values as a function of time could be employed to monitor the oxidation of the studied compounds by hydrogen peroxide in the presence of HRP. Thus, under the tested experimental conditions, absorbances at 485 and 275 nm were employed to monitor the concentration of OII, phenol, or BPA, respectively.

3.2. Oxidation of Orange II (OII). *3.2.1. Pulse Experiments.* Preliminary batch experiments were performed in order to observe the evolution of ORP profiles obtained during the oxidation of OII (0.17 mM) with hydrogen peroxide (0.21 mM) at pH 9 catalyzed by HRP (30 mg/L). At the beginning of the experiment, OII and HRP were both present in the reaction mixture. Figure 2a shows that the absorbance at 485 nm was 3.2 and it remained constant. Then, after the first addition of hydrogen peroxide (t = 0), absorbance values decreased to 0.14 within the first 6 min. At this time, almost a complete decolorization was achieved, and the decolorization reaction was halted. Figure 2b shows the ORP profile corresponding to the reaction mixture. Prior to the addition of hydrogen peroxide, ORP values were almost constant at 120 mV. When hydrogen peroxide was added (t = 0), the oxidation reaction started and a quite noticeable increase of ORP was observed. ORP values reached a maximum value of 170 mV close to the time at which the decolorization reaction ceased. According to Figure 2c, the time at which ORP reached this maximum value can be easily obtained by means of the derivative of ORP as a function of time. At t = 15 min, while OII was depleted, a second addition of hydrogen peroxide was performed, yet ORP values continued decreasing. Then the addition of OII at t = 30 min triggered the increase of ORP from 140 mV up to a maximum value of about 180 mV. Once again, the time corresponding to this maximum ORP was close to the end of the decolorization reaction (Figure 2b).

The results shown in Figure 2 clearly indicated that the increase of ORP values was associated with the enzymatic activity rather than the sole presence of hydrogen peroxide or OII. Namely, when the enzyme was in contact only with OII, ORP values remained about 120 mV. Then, after the addition of hydrogen peroxide (t = 0 min), the decolorization reaction started and ORP increased. However, the second addition of hydrogen peroxide (t = 15 min) did not cause a new increase of ORP because OII was depleted. Finally, at t = 30 min, the addition of the reducing substrate (OII) started a new

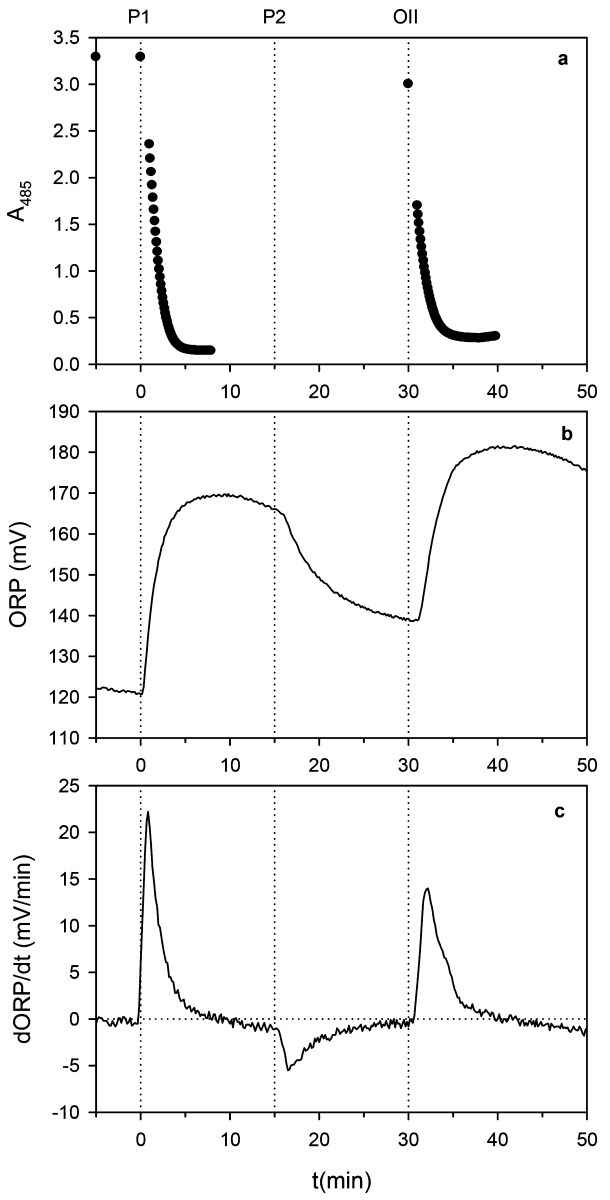

Figure 2. Example of a decolorization reaction of OII (0.17 mM) by hydrogen peroxide (0.21 mM) catalyzed by HRP (30 mg/L) at pH 9 in buffer phosphate (100 mM): (a) absorbance at 485 nm (A_{485}), (b) ORP, and (c) the derivative of ORP as a function of time (dORP/dt). Dotted lines indicate the time at which hydrogen peroxide or OII was added.

decolorization reaction catalyzed by the enzyme. These results demonstrate that the increase in ORP values was triggered by the enzyme activity. Conversely, when the enzyme was not active (e.g., when one substrate was absent) ORP values slowly decreased.

3.2.2. Fed-Batch Experiments. Fed-batch experiments were performed to decolorize solutions of OII. In these experiments, the initial HRP and OII concentrations were 30 mg/L and 0.19 mM, respectively. The reaction was started by the continuous addition of hydrogen peroxide (1.8 mM) at different flow rates (0.21−2.37 mL/min). In all cases, the initial volume was 250 mL, pH = 9, and the ORP signal was employed to monitor decolorization experiments and to determine the reaction end point.

DOI: 10.1021/acs.iecr.8b04616
Ind. Eng. Chem. Res. XXXX, XXX, XXX−XXX

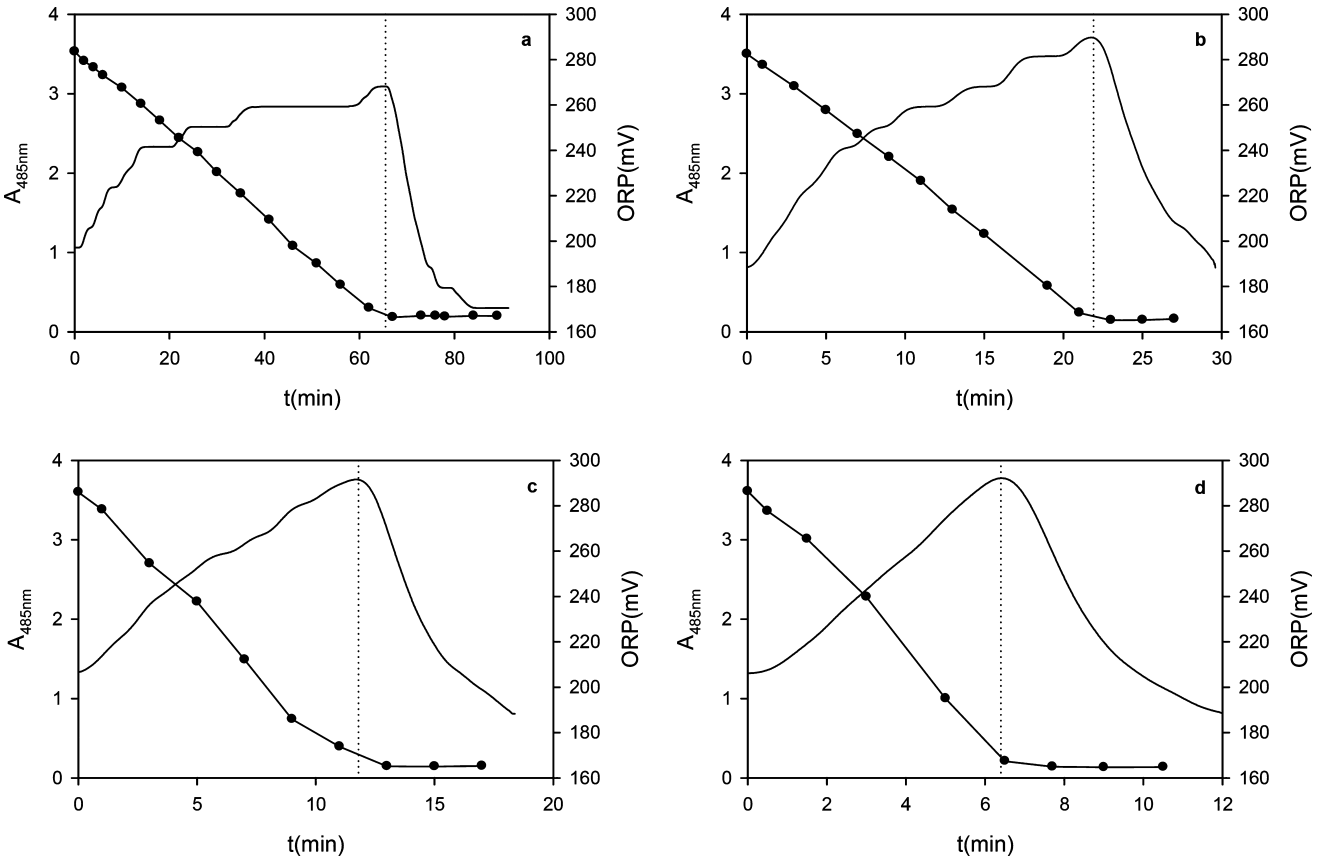

Figure 3. Changes of absorbance at 485 nm (A_{485}) and ORP during the decolorization of OII solutions (0.19 mM) by the continuous addition of hydrogen peroxide (1.8 mM) at the following flow rates (mL/min): (a) 0.21, (b) 0.65, (c) 1.28, and (d) 2.37. Dotted lines indicate the critical time (t_C). In all cases, the concentration of HRP was 30 mg/L, pH = 9, and the initial volume was 250 mL.

Figure 3 shows the change of absorbance at 485 nm (A_{485}) and ORP during the decolorization reaction. In all cases, a linear decrease of A_{485} was observed, with the decolorization rate proportional to the employed flow rate. If the addition of hydrogen peroxide was ceased then the decolorization stopped immediately, demonstrating that under the tested conditions the accumulation of hydrogen peroxide was negligible. Absorbances reached a minimum value at a given critical time (t_C), and then they remained constant. As was discussed previously, this critical time (t_C) represents the end of the decolorization reaction. In all cases depicted in Figure 3, obtained t_C were similar to the time at which ORP reached a maximum value (Table 1). These ORP-based t_C values were obtained from the plot of the first derivative of ORP as a function of time (Figure S2). It must be noted that because ORP was measured on a continuous basis, a more accurate estimation of t_C was obtained using ORP in comparison with the assessment of t_C using absorbance values.

Table 1. Results Obtained in Fed-Batch Experiments To Oxidize OII[a]

run	Q_{in} (mL/min)	$[OII]_0$ (mM)	t_C (min)	$t_{C(ORP)}$ (min)	Y_S[b] (mol/mol)
1	0.21	0.183	67	65	1.83
2	0.65	0.183	24	22	1.65
3	1.28	0.187	13	12	1.55
4	2.37	0.187	7	6	1.54

[a]In all cases, the inlet hydrogen peroxide concentration (H_2O_{2in}) was 1.8 mM, pH = 9, E_T = 30 mg/L, and the initial volume (V_0) was 250 mL. [b]Amount of hydrogen peroxide consumed: $Y_S = \frac{V_0[OII]_0}{Q_{in}H_2O_{2in}t_{C(ORP)}}$

Table 1 shows that the amount of hydrogen peroxide consumed to decolorize OII (Y_S) decreased as Q_{in} increased. This effect can be attributed to the fact that during a fed-batch the hydrogen peroxide concentration increases as a function of Q_{in}. However, because the decomposition of hydrogen peroxide to water and oxygen increased with the concentration of hydrogen peroxide,[13] the higher Q_{in} gave lower Y_S. For more details, see the Supporting Information, item 3.

In summary, the results displayed in Figure 3 show that the ORP signal can be used to determine the end point of the oxidation of OII by hydrogen peroxide catalyzed by HRP. However, these results could be applicable only to OII. For this reason, to evaluate the effectiveness of the ORP signal to detect the end point of the oxidation reaction of other xenobiotics, phenol and BPA were also tested as reducing substrates.

3.3. Comparison between Different Reducing Substrates. Figure 4 shows the comparison between the oxidation kinetics corresponding to the different tested reducing substrates (OII, phenol, and BPA). Table 2 shows experimental conditions and main results. It must be noted that the time scale of these experiments ranged from 70 to 130 min. Thus, to aid the comparison between the different experiments, the results in Figure 4 were plotted as a function of a normalized time, represented by the ratio t/t_C. In all cases, the critical time (t_C) was obtained from the plot of the derivative of ORP as a function of time (see Figure S3). Table

DOI: 10.1021/acs.iecr.8b04616
Ind. Eng. Chem. Res. XXXX, XXX, XXX−XXX

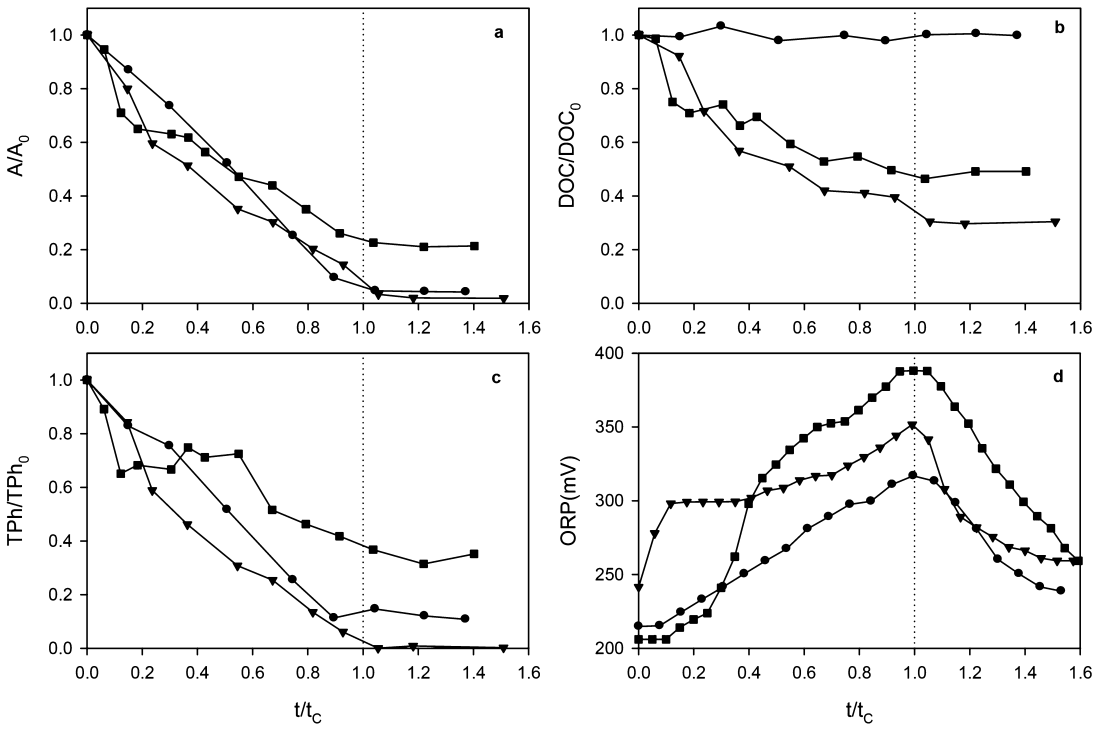

Figure 4. Change of (a) absorbance, (b) dissolved organic carbon (DOC), (c) total phenols (TPh), and (d) ORP as a function of the normalized time (t/t_C) during the oxidation of OII (circles), phenol (triangles), and BPA (squares) in the presence of HRP by the continuous addition of hydrogen peroxide. For OII, absorbance was measured at 485 nm. Absorbances corresponding to phenol and BPA were measured at 275 nm. See Table 2 for more details concerning the experimental conditions.

Table 2. Comparison between Y_S Values Corresponding to the Different Tested Reducing Substrates (S)[a]

substrate	Q_{in} (mL/min)	$[S]_0$ (mM)	t_C (min)	$t_{C(ORP)}$ (min)	Y_S[b] (mol/mol)
OII	0.43	0.20	35	31	1.84
phenol	0.73	0.50	58	55	1.64
BPA	0.37	0.48	85	82	2.20

[a]In all cases, the inlet hydrogen peroxide concentration (H_2O_{2in}) was 1.8 mM, pH = 8, E_T = 20 mg/L, and the initial volume (V_0) was 250 mL. [b]Amount of hydrogen peroxide consumed: $Y_S = \frac{V_0[S]_0}{Q_{in}H_2O_{2in}t_{C(ORP)}}$

2 shows the obtained critical times (t_C) corresponding to the tested reducing substrates.

Figure 4 shows that absorbance values (Figure 4a) and total phenols concentrations (Figure 4c) exhibited a similar trend. In both cases, these measurements decreased as a function of the normalized time, reaching constant values at $t/t_C \geq 1$. In addition, Figure 4b shows that in the case of OII, DOC values remained constant, indicating that the reducing substrate (OII) and the oxidation products remained in the aqueous phase. Conversely, in the case of phenol and BPA, DOC removals were 70 and 50%, respectively. For all of the tested compounds, Figure 4d shows that ORP reached a maximum value when the oxidation reaction halted. Moreover, the addition of an excess of hydrogen peroxide caused a quite noticeable decrease of ORP values.

According to Table 2, the amount of substrate removed per mole of hydrogen peroxide added ranged between 1.6 and 2.2 mol/mol. These values are higher than those reported by other authors in batch systems. For example, several authors reported a ratio of Y_S close to 1 mol/mol for the removal of phenol by HRP.[25−28] Chahbane et al.[29] reported values that ranged from 0.5 to 1 mol/mol.

Figure 5 shows the change of UV/vis spectra during the oxidation of OII, phenol, and BPA by hydrogen peroxide in the presence of HRP. As a general rule, a decrease of the OII characteristic absorbance bands within the visible region was observed. However, as the reaction proceeds a new absorption band at 340 nm appeared due to the formation of OII oxidation products which cannot be further oxidized under the tested conditions. According to Cabrera et al.,[8] these OII oxidation products are a mixture of 1-amino-2-naphthol, sulfanilate, 1-diazo-2-naphthol, 1,2-naphthoquinone, 4-hydroxybenzenesulfonate, 4-diazobenzenesulfonate, and aniline.

When phenol or BPA were tested as the reducing substrates, the formation of a dark-brown or a white precipitate, respectively, was observed. It must be noted that the presence of precipitates due to the polymerization of phenolic compounds by HRP was reported by several authors.[30−33] In our experiments, these precipitates were removed by centrifugation and filtration of the reaction mixture prior the measurement of DOC. Thus, the decrease of DOC values observed during the oxidation of phenol and BPA could be attributed to the formation of these insoluble polymerization products rather than their complete oxidation to CO_2.

The change of the UV/vis spectrum corresponding to OII (Figure 5a) contrast with those obtained when phenol and BPA were tested (Figure 5b,c). In the latter cases, the shape of the obtained UV/vis spectra was almost constant as a function of time. Thus, the changes of UV/vis spectra were in accordance with a decrease of phenol and BPA concentrations with a slight formation of soluble oxidation products. These oxidation products were responsible for the DOC values at the end of the oxidation reaction (Figure 4b). Moreover, the

DOI: 10.1021/acs.iecr.8b04616
Ind. Eng. Chem. Res. XXXX, XXX, XXX−XXX

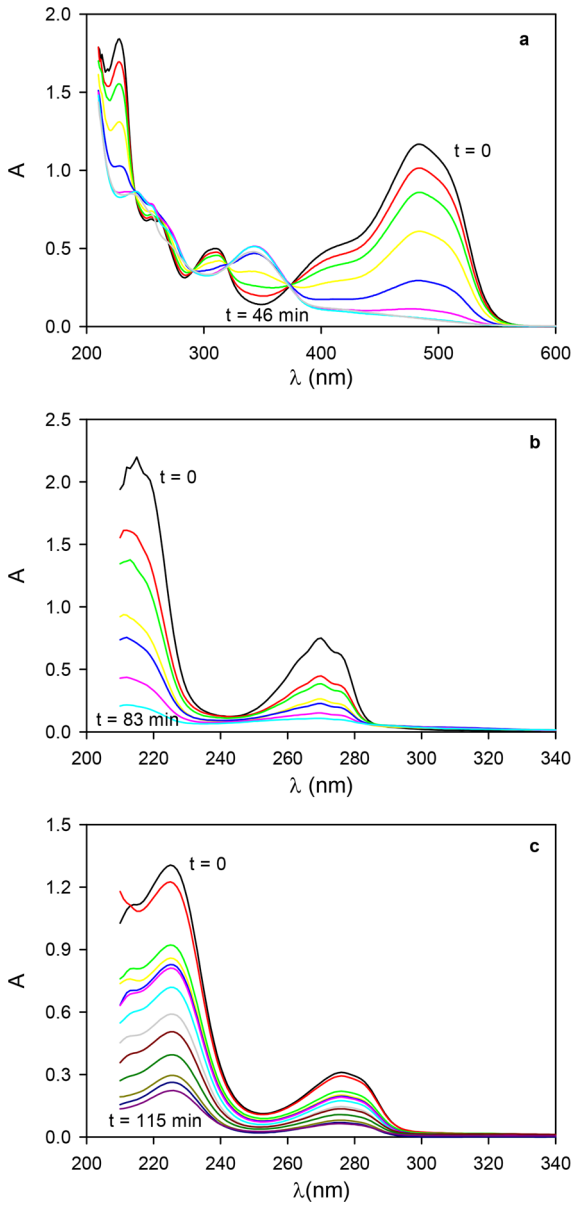

Figure 5. UV/vis spectral changes during the oxidation of (a) OII, (b) phenol, and (c) BPA. See Table 2 for details concerning the experimental conditions.

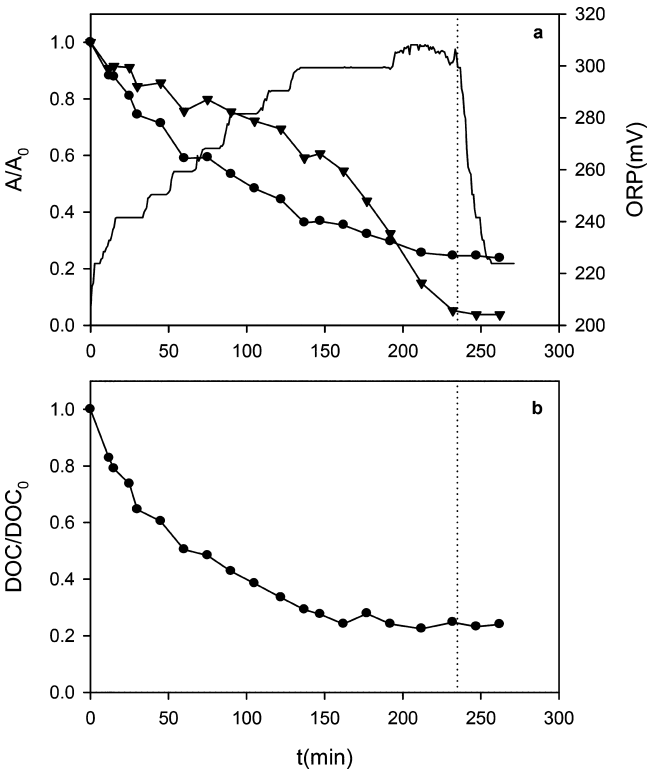

Figure 6. Oxidation of a binary mixture composed by OII (0.2 mM) and BPA (0.5 mM) by the continuous addition of hydrogen peroxide (1.8 mM) at 0.20 mL/min. The initial concentration of HRP was 20 mg/L, pH = 8 (phosphate buffer, 100 mM), and the initial volume was 250 mL. (a) Normalized absorbances at 275 nm (circles) and 485 nm (triangles) and ORP values (line). (b) Normalized DOC concentration. Vertical dotted lines indicate the critical time.

results depicted in Figures 4 and 5 demonstrate that these products cannot be further oxidized under the tested experimental conditions.

3.4. Oxidation of the Binary Mixture OII−BPA. The results shown in Figures 3 and 4 demonstrate that the ORP signal can be used to detect the end point of the oxidation of single compounds by hydrogen peroxide catalyzed by HRP. To verify the applicability of the ORP in more complex reaction systems, the oxidation of a binary mixture composed by OII (0.2 mM) and BPA (0.5 mM) was studied. In this experiment, hydrogen peroxide (1.8 mM) was continuously added at 0.20 mL/min, the initial concentration of HRP was 20 mg/L, and pH = 8.

Figure 6a shows the change of absorbances (A) at 275 and 485 nm, normalized with respect to their initial values, as a function of time. It must be noted that according to Figures 1 and 5, OII and its oxidation products in a minor extent were responsible for the absorbance at 485 nm. For example, Figure 5a shows that if the initial absorbance corresponding to OII was about 1.2, after the decolorization reaction the absorbance decreased to 0.05. This residual absorbance was due to the presence of OII oxidation products. Moreover, Figures 1 and 5b demonstrate that at 485 nm the absorbance corresponding to BPA was negligible. Conversely, the absorbance at 275 nm was the result of the presence of OII, BPA, and their corresponding oxidation products. However, Figure 5a shows that at this wavelength the change of absorbance during to the oxidation of OII was negligible. In the example depicted in Figure 5a, the initial absorbance corresponding to OII was 0.42 while at the end of the experiment the absorbance was 0.47. For this reason, the change of absorbance at 275 nm was attributed mainly to the change of the BPA concentration during the oxidation reaction.

Figure 6b shows that during the oxidation of the mixture OII−BPA, DOC values decreased as a function of time. It must be noted that when the oxidation of OII was studied, DOC values remained constant. Conversely, a noticeable decrease in DOC values due to the formation of an insoluble product was obtained when BPA was studied (Figure 4b). During the oxidation of the mixture OII−BPA, the change of the absorbance at 275 nm (Figure 6a) was similar to the variation of DOC values as a function of time (Figure 6b), confirming that the change of absorbance at 275 nm represented the change of the BPA concentration in the mixture.

DOI: 10.1021/acs.iecr.8b04616
Ind. Eng. Chem. Res. XXXX, XXX, XXX−XXX

During the first 150 min, the absorbance at 485 nm decreased as a function of time (Figure 6a). Because at this wavelength the absorbance corresponding to BPA was negligible, this result indicates that some OII was removed from the solution. It must be mentioned that during the oxidation of the mixture OII−BPA the formation of a reddish orange insoluble product was observed. Taking into account that the formation of a white precipitate was observed when BPA alone was studied, it can be concluded that the reddish orange color of the precipitate formed during the oxidation of the mixture OII−BPA was due to the presence of OII in the precipitate. Thus, the decrease in absorbance at 485 nm during the first 150 min can be attributed to the OII consumption due to the formation of this reddish-orange precipitate. For reaction times higher than 150 min, absorbance at 275 nm and DOC values were almost constant, indicating the completion of the oxidation of BPA. Under these conditions, the absorbance at 485 nm rapidly decreased (Figure 6), suggesting that HRP first catalyzed the oxidation of BPA and then the oxidation of OII. It must be noted that Figure 6a shows that ORP changes also exhibited two phases. During the first 150 min, a noticeable increase of ORP values from 210 to about 300 mV was observed. This phase corresponded to the removal of BPA and OII by co-precipitation. Then, from 150 to 230 min a slight increase of ORP values and a quite noticeable decrease of the absorbance at 485 nm were obtained, corresponding to the oxidation of OII. Finally, at 230 min OII was exhausted, and consequently, ORP values decreased. Thus, it can be concluded that the ORP signal can also be employed to detect the end point of the oxidation reaction of a binary mixture composed by OII and BPA catalyzed by HRP.

4. CONCLUSIONS

In this work, the use of ORP measurements to detect the end point of the oxidation of three model pollutants (orange II, phenol, BPA) using hydrogen peroxide catalyzed by HRP was studied. The obtained results demonstrate that ORP values increased only when both substrates of the enzyme (hydrogen peroxide and the target compound) were present in the reaction mixture. For all of the tested pollutants, the time at which ORP reached a maximum value was close to the end of the oxidation reaction. The maximum ORP value could be easily detected by means of the derivative of ORP as a function of time (dORP/dt). In all cases, when hydrogen peroxide was added in excess, a decrease of ORP values was observed. This behavior was also observed during the oxidation of a mixture of OII and BPA. This work demonstrates that ORP can be useful to control the addition of hydrogen peroxide during the oxidation of OII, phenol, and BPA catalyzed by HRP, minimizing time and process costs.

■ ASSOCIATED CONTENT

Supporting Information

The Supporting Information is available free of charge on the ACS Publications website at DOI: 10.1021/acs.iecr.8b04616.

Absorption spectra obtained under the minimum tested concentrations of OII, BPA, and phenol and maximum hydrogen peroxide and HRP concentrations (Figure S1); evaluation of the critical time (t_C) of Figure 2 (Figure S2); pseudo-steady-state concentration of hydrogen peroxide in a fed-batch (mathematical topic); evaluation of the critical time (t_C) of Figure 4 (Figure S3) (PDF)

■ AUTHOR INFORMATION

Corresponding Author

*E-mail: edgardo.contreras@fi.mdp.edu.ar.

ORCID

E. M. Contreras: 0000-0003-0546-1095

Notes

The authors declare no competing financial interest.

■ ACKNOWLEDGMENTS

The authors gratefully acknowledge financial support from Consejo Nacional de Investigaciones Científicas y Técnicas (CONICET), Universidad Nacional de la Plata (UNLP), and Agencia Nacional de Promoción Científica y Tecnológica (ANPCyT), Argentina.

■ REFERENCES

(1) Rauf, M. A.; Salman Ashraf, S. Survey of recent trends in biochemically assisted degradation of dyes. *Chem. Eng. J.* **2013**, *209*, 520.

(2) Ali, L.; Algaithi, R.; Habib, H. M.; Souka, U.; Rauf, M. A.; Ashraf, S. S. Soybean peroxidase-mediated degradation of an azo dye - a detailed mechanistic study. *BMC Biochem* **2013**, *14*, 35.

(3) Saratale, R. G.; Saratale, G. D.; Chang, J. S.; Govindwar, S. P. Bacterial decolorization and degradation of azo dyes: A review. *J. Taiwan Inst. Chem. Eng.* **2011**, *42*, 138.

(4) Agarwal, P.; Gupta, R.; Agarwal, N. A Review on Enzymatic Treatment of Phenols in Wastewater. *J. Biotechnol. Biomater.* **2016**, *6*, 1.

(5) Franciscon, E.; Piubeli, F.; Garboggini, F. F.; De Menezes, C. R.; Silva, I. S.; Paulo, A. C.; Grossman, M. J.; Durrant, L. R. Polymerization study of the aromatic amines generated by the biodegradation of azo dyes using the laccase enzyme. *Enzyme Microb. Technol.* **2010**, *46*, 360.

(6) Chiong, T.; Lau, S.; Lek, Z. H.; Koh, B. Y.; Danquah, M. K. Enzymatic treatment of methyl orange dye in synthetic wastewater by plant-based peroxidase enzymes. *J. Environ. Chem. Eng.* **2016**, *4*, 2500.

(7) Sahare, P.; Ayala, M.; Vazquez-Duhalt, R.; Pal, U.; Loni, A.; Canham, L. T.; Osorio, I.; Agarwal, V. Enhancement of peroxidase stability against oxidative self-inactivation by co-immobilization with a redox-active protein in mesoporous silicon and silica microparticles. *Nanoscale Res. Lett.* **2016**, *11*, 417.

(8) Cabrera, C.; Cornaglia, A.; Córdoba, A.; Magario, I.; Ferreira, M. L. Kinetic modelling of the hematin catalysed decolourization of Orange II solutions. *Chem. Eng. Sci.* **2017**, *161*, 127.

(9) Dunford, H. B.; Stillman, J. S. On the function and mechanism of action of peroxidases. *Coord. Chem. Rev.* **1976**, *19*, 187.

(10) Kalsoom, U.; Ashraf, S. S.; Meetani, M. A.; Rauf, M. A.; Bhatti, H. N. Mechanistic study of a diazo dye degradation by soybean peroxidase. *Chem. Cent. J.* **2013**, 93.

(11) Nicell, J. A.; Wright, H. A model of peroxidase activity with inhibition by hydrogen peroxide. *Enzyme Microb. Technol.* **1997**, *21*, 302.

(12) Jakopitsch, C.; Wanasinghe, A.; Jantschko, W.; Furtmuller, P. G.; Obinger, C. Kinetics of Interconversion of Ferrous Enzymes, Compound II and Compound III, of Wild-type *Synechocystis* Catalase-peroxidase and Y249F. Proposal for the catalatic mechanism. *J. Biol. Chem.* **2005**, *280*, 9037.

(13) Morales Urrea, D. A.; Haure, P. M.; García Einschlag, F. S.; Contreras, E. M. Horseradish peroxidase-mediated decolourization of Orange II: modelling hydrogen peroxide utilization efficiency at different pH values. *Environ. Sci. Pollut. Res.* **2018**, *25*, 19989.

DOI: 10.1021/acs.iecr.8b04616
Ind. Eng. Chem. Res. XXXX, XXX, XXX−XXX

(14) Contreras, E. M.; Bertola, N. C.; Zaritzky, N. E. Monitoring the Ozonation of Phenol Solutions at Constant pH by Different Methods. *Ind. Eng. Chem. Res.* **2011**, *50*, 9799.
(15) Yu, R.-F.; Chen, H.-W.; Cheng, W.-P.; Lin, Y.-J.; Huang, C.-L. Monitoring of ORP, pH and DO in heterogeneous Fenton oxidation using nZVI as a catalyst for the treatment of azo-dye textile wastewater. *J. Taiwan Inst. Chem. Eng.* **2014**, *45*, 947.
(16) Vitale, A. A.; Bernatene, E. A.; Vitale, M. G.; Pomilio, A. B. New Insights of the Fenton Reaction Using Glycerol as the Experimental Model. Effect of O_2, Inhibition by Mg^{2+}, and Oxidation State of Fe. *J. Phys. Chem. A* **2016**, *120*, 5435.
(17) Kishimoto, N.; Hatta, M.; Kato, M.; Otsu, H. Effects of oxidation−reduction potential control and sequential use of biological treatment on the electrochemical Fenton-type process. *Process Saf. Environ. Prot.* **2017**, *105*, 134.
(18) Vongvichiankul, C.; Deebao, J.; Khongnakorn, W. Relationship between pH, Oxidation Reduction Potential (ORP) and Biogas Production in Mesophilic Screw Anaerobic Digester. *Energy Procedia* **2017**, *138*, 877.
(19) Foladori, P.; Petrini, S.; Andreottola, G. Evolution of real municipal wastewater treatment in photobioreactors and microalgae-bacteria consortia using real-time parameters. *Chem. Eng. J.* **2018**, *345*, 507.
(20) Lackner, S.; Horn, H. Evaluating operation strategies and process stability of a single stage nitritation−anammox SBR by use of the oxidation−reduction potential (ORP). *Bioresour. Technol.* **2012**, *107*, 70.
(21) Weißbach, M.; Drewes, J. E.; Koch, K. Application of the oxidation reduction potential (ORP) for process control and monitoring nitrite in a Coupled Aerobic-anoxic Nitrous Decomposition Operation (CANDO). *Chem. Eng. J.* **2018**, *343*, 484.
(22) Modaressi, K.; Taylor, K. E.; Bewtra, J. K.; Biswas, N. Laccase-catalyzed removal of bisphenol-A from water: Protective effect of PEG on enzyme activity. *Water Res.* **2005**, *39*, 4309.
(23) Li, F.; Li, G.; Zhang, X. Mechanism of enhanced removal of quinonic intermediates during electrochemical oxidation of Orange II under ultraviolet irradiation. *J. Environ. Sci.* **2014**, *26*, 708.
(24) Zhou, G.; Guo, J.; Zhou, G.; Wan, X.; Shi, H. Photodegradation of Orange II using waste paper sludge-derived heterogeneous catalyst in the presence of oxalate under ultraviolet light emitting diode irradiation. *J. Environ. Sci.* **2016**, *47*, 63.
(25) Buchanan, I. D.; Nicell, J. A. Model development for horseradish peroxidase-catalyzed removal of aqueous phenol. *Biotechnol. Bioeng.* **1997**, *54*, 251.
(26) Buchanan, I. D.; Nicell, J. A. A simplified model of peroxidase-catalyzed phenol removal from aqueous solution. *J. Chem. Technol. Biotechnol.* **1999**, *74*, 669.
(27) Wu, J.; Taylor, K. E.; Biswas, N.; Bewtra, J. K. Kinetic model for removal of phenol by horseradish peroxidase with PEG. *J. Environ. Eng.* **1999**, *125*, 451.
(28) Buchanan, I. D.; Han, Y. S. Assessment of the potential of *Arthromyces ramosus* peroxidase to remove phenol from industrial wastewaters. *Environ. Technol.* **2000**, *21*, 545.
(29) Chahbane, N.; Popescu, D. L.; Mitchell, D. A.; Chanda, A.; Lenoir, D.; Ryabov, A. D.; Schramm, K. W.; Collins, T. J. FeIII−TAML-catalyzed green oxidative degradation of the azo dye Orange II by H2O2 and organic peroxides: products, toxicity, kinetics, and mechanisms. *Green Chem.* **2007**, *9*, 49.
(30) Ayyagari, M.; Akkara, J. A.; Kaplan, D. L. Enzyme-mediated polymerization reactions: peroxidase-catalyzed polyphenol synthesis. *Acta Polym.* **1996**, *47*, 193.
(31) Valderrama, B.; Ayala, M.; Vazquez-Duhalt, R. Suicide Inactivation of Peroxidases and the Challenge of Engineering More Robust Enzymes. *Chem. Biol.* **2002**, *9*, 555.
(32) Tonami, H. Oxidative Polymerization of Phenolic Compounds Catalyzed by Peroxidase and Its Model Complex. Ph.D. Thesis, Kyoto University, 2003.
(33) Gómez, J. L.; Bódalo, A.; Gómez, E.; Bastida, J.; Hidalgo, A. M.; Gómez, M. A covered particle deactivation model and an expanded Dunford mechanism for the kinetic analysis of the immobilized SBP/phenol/hydrogen peroxide system. *Chem. Eng. J.* **2008**, *138*, 460.

DOI: 10.1021/acs.iecr.8b04616
Ind. Eng. Chem. Res. XXXX, XXX, XXX−XXX